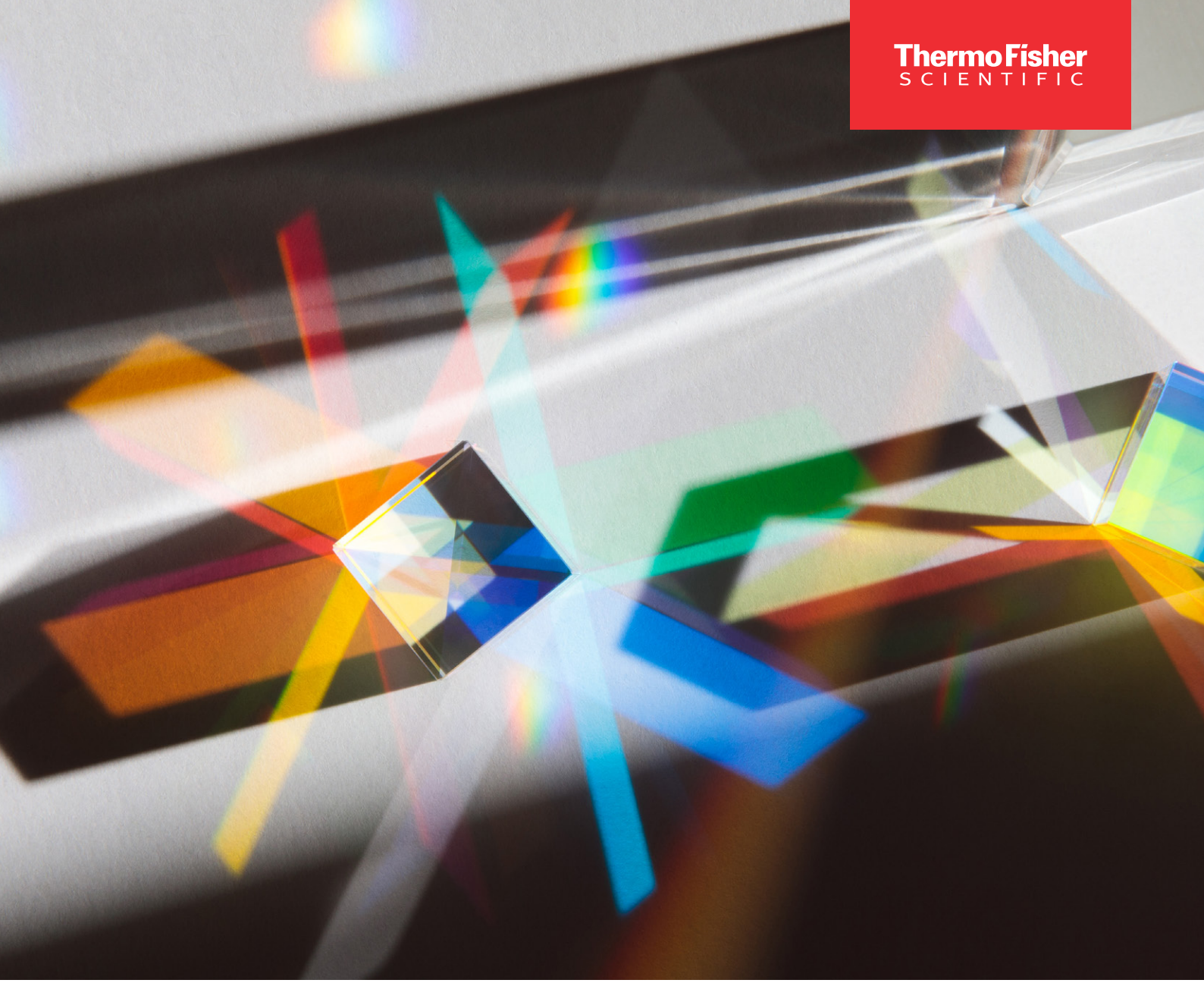

Solid-State Materials

Analysis Through UV-Visible Spectroscopic Techniques

thermo scientific

Introduction

The application notes in this compendium show the versatility and dependability of Thermo Scientific™ Evolution™ UV-Visible Spectrophotometers. These instruments are effective in measuring the reflection, absorption, and transmission properties of solid materials like films, powders, and curved lenses.

The interaction of ultraviolet and visible light with solid materials generates valuable information about the properties and potential utility of those materials. By analyzing the degree to which light scatters off the irregular surface of a powder, or how rays of light pass through the shaped lens of an eyeglass, the real-world effectiveness of these materials can be quantified.

The usefulness of UV-Vis spectroscopic analysis can be applied to semiconductors as well. For example, the unique electronic structure of a semiconducting material results in a specific “band gap” energy. The size of this band gap can have implications for a variety of photo-induced applications (e.g., photovoltaics). Because UV-Visible absorption and reflectance spectra arise from transitions between states on either side of that band gap, these spectral measurements can be directly used to estimate the band gap energy.

Additional accessories that are compatible with Evolution spectrophotometers allow for the gathering of detailed information about specific aspects of the test substance. For instance, in the case of curved lenses, the use of an integrating sphere in conjunction with a detector delivers useful UV-Visible spectra with high sensitivity; the transmittance and reflectance data collected this way can indicate if a small fraction of light is absorbed, or perhaps if a miniscule amount of a chromophore is present in the lens being analyzed. In another example, when investigating a solid thin film such as a monitor’s privacy screen, a UV-Vis spectrophotometer combined with a variable angle Specular Reflectance Accessory (SRA) can demonstrate the effectiveness of the film in preventing surreptitious viewing from a side angle.

The four applications described herein showcase the Evolution line of UV-Visible spectrophotometers. The instruments have demonstrated their ability to perform routine measurements and generate high resolution data while providing experimental flexibility for research and more complex applications.

Contents

Application note

Solid-State Materials: Analysis Through UV-Visible Spectroscopic Techniques

UV-Visible techniques are used to observe how a substance behaves when irradiated with light in the UV and visible range of the electromagnetic spectrum. Possible interactions include transmission of light through the material, reflection off the surface of the sample, and absorption of the light by the material. Absorption measurements are by far the most common method for analyzing UV-Visible data as this value can be linearly correlated to the concentration of a given analyte through Beer's law (eqn. 1), where A is the absorbance of the sample, c is the concentration, l is the pathlength by which the light passes through, and ε is the extinction coefficient unique to the analyte measured. Often, UV-Visible absorption methods are used to analyze solution-phase samples, however, solid-state samples can also be readily measured using a variety of UV-Visible techniques.

$$A = cl\varepsilon$$

Equation 1.

The same principles which govern solution-phase samples also apply to solid-state substances, however there are a few major differences between the two sample types which must be considered when working with solid samples. Herein, we aim to discuss a few of the different possible analyses which can be performed on solid samples as well as the inherent considerations that must be accounted for when analyzing these materials.

First, unlike in solutions, reflections are often not negligible in solid-phase samples, and thus different methods of analysis are required. The reflection spectrum can contain valuable information about a given solid, including the color of a non-transmissive material or the usable reflective range for a mirror or coating. As such, reflection measurements of solids are not uncommon.

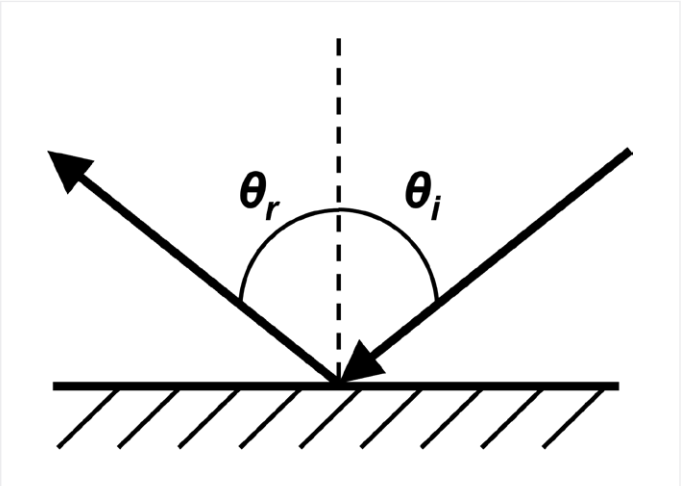

Figure 1. Diagram depicting angle of reflectance (θ_r) and angle of incidence (θ_i).

Reflections in spectroscopy can be defined as the redirection of light by a material at an angle (θ_r) equivalent to the angle of incidence (θ_i) as shown in Figure 1. There are two different forms of reflections possible when light interacts with the surface of a material: specular and diffuse. Specular reflections (Figure 2a) are mirror-like in nature.[1,2] These reflections involve the uniform reflection of light off the sample surface. Substances with more uniform surfaces are likely to be specular reflectors.

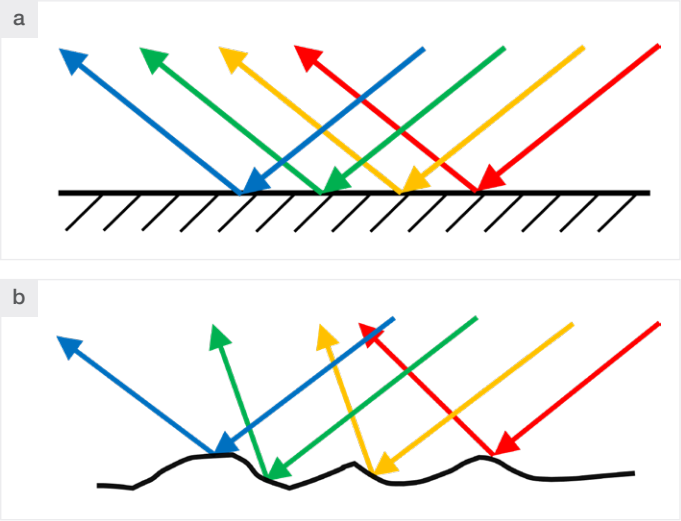

Figure 2. Example of (a) specular reflections off an ideal, uniform surface and (b) diffuse reflections off an irregular, nonuniform surface.

As an example, privacy screens (films for smart devices) can specularly reflect light. This film functions such that when viewed directly, light can be transmitted through the screen and can be seen, however when viewed from an angle, the screen appears black and light is either absorbed or reflected, protecting the user's privacy.[3,4] This material will inherently have an angle-dependent response to incidient light—a response which is important to monitor for QA/QC purposes. For these systems, it is important to measure the full reflection spectrum, as well as transmission spectrum, as a function of the angle of incidence. Figure 3 includes the specular reflectance spectra for a commercially available privacy screen. As would be expected, the recorded reflectance is higher for samples when the angle of incidence is wider compared to near-normal specular reflectance.

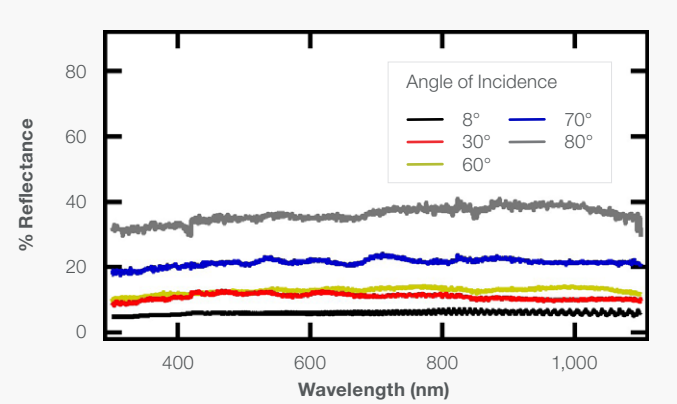

Figure 3. Specular Reflectance spectra of a privacy screen collected at different angles of incidence. Spectra were collected using the Thermo Scientific™ Evolution™ Pro UV-Visible spectrophotometer equipped with the VeeMAX variable angle specular reflectance accessory (30˚ – 80˚ angles of incidence) and 8˚ specular reflectance accessory.

Diffuse reflections are more irregular and typically arise from non-uniform or "rough" surfaces of a solid material (Figure 2b).[1,2] These reflections are often present with powdered samples or with opaque film samples, and are akin to scattering events in solutions where light is scattered in non-uniform directions. As with scattering events, the irregular direction of the light can cause this signal to be directed away from the instrument detector, resulting in a falsely low reflectance signal. These abnormalities can be corrected for if using the appropriate accessory (e.g., an integrating sphere).

Nanoparticles and nanomaterials are often analyzed in the solid phase, including as films or powders, using UV-Visible spectroscopy. Reflections of these substances, particularly powders, are typically diffuse as the surfaces of the film or particles are often irregular. As an example, Figure 4 includes the reflection spectra of TiO_2 nanoparticles of varying crystal structure. For semiconductors like TiO_2, changes in the reflection or absorption spectrum observed for samples of differing crystal structure can have implications for the electronic structure of a given material. Thus, UV-Visible analysis can be a helpful tool for materials characterization.[5-7]

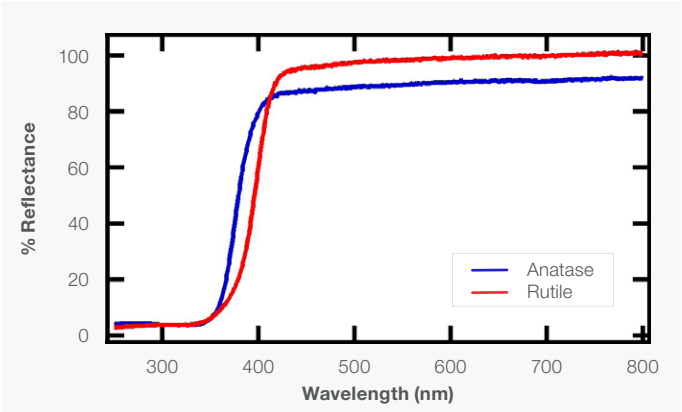

Figure 4. Reflectance spectra of anatase (blue) and rutile (red) TiO_2 collected using the ISA-220 and Thermo Scientific™ Evolution™ One Plus UV-Visible spectrophotometer.

In addition to films and powders, solid samples can also be made with different, non-uniform shapes. For example, some materials, like lenses for eyeglasses, have curved instead of flat surfaces. Due to refraction, these curved materials cause incident light to be transmitted in a non-collimate manner. Similar to diffuse reflections, the converging or diverging beam may not be able to reach the detector, requiring the use of an integrating sphere to properly direct the light to the detector. As an example, Figure 5 includes the reflectance and transmittance spectra of a blue light reduction eyeglass lens, acquired using an integrating sphere (ISA-220). Here, the ISA-220 is able to direct the light uniformly toward the detector, preventing the loss of light that does not transmit through the sample as a collimated beam.

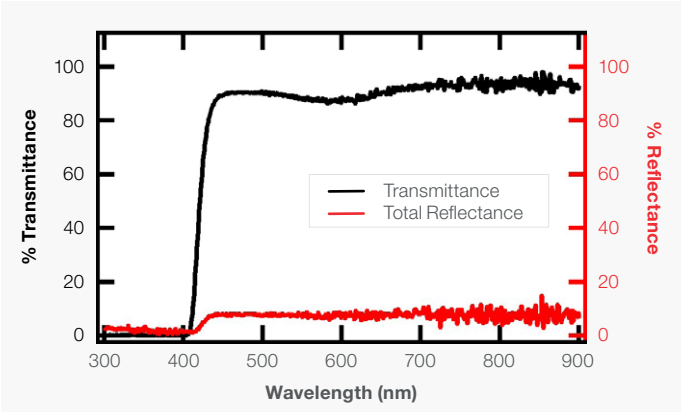

Figure 5. Transmittance (black) and Reflectance (red) spectra for a blue light reduction lens collected using the ISA-220 and Thermo Scientific™ Evolution™ One Plus UV-Visible spectrophotometer.

In addition to more prevalent contributions from reflections, the loss of degrees of freedom in the solid phase as compared to solutions can influence measurements in ways not observed for the latter sample type. Unlike in solutions where Brownian motion allows for the movement and mixing of compounds, leading to a homogeneous sample, solids can be fairly heterogeneous in nature. Under these circumstances, the amount of an analyte of interest present in a given sample can be highly spatially dependent, leading to differences in an observed spectrum from spot to spot. Furthermore, the rigidity of the material prevents the rotation of compounds within the solid matrix, leading to orientation-dependent effects on the collected UV-Visible spectrum not observed in solution-phase systems.

Tips and Tricks for Measuring Solid-State Materials with UV-Visible Techniques

As described previously, there are many different considerations which must be accounted for when studying solid-state materials. Below is a list of common tips and tricks that can help when studying solid substances.

- Unlike with solution-phase measurements, solid state materials can be highly heterogeneous. If repeat measurements are to be taken at different times or on different days, ensure the same spot is sampled to avoid errors due to spatial differences in the material's composition.
  - If there is concern about sample heterogeneity, it can be helpful to run the same sample in triplicate to determine an average spectrum. For films, choose different sampling regions on the same film. For powders, sample separate portions, allowing for mixing in between each replicate collection.

- For film measurements, the substrate is highly important in establishing the material's background for transmission measurements. Be sure to use a substrate which does not absorb greatly in the spectral region of interest for the sample. If the substrate absorbs too much, additional information cannot be obtained concerning the transmission of the sample alone.
  - If the spectrum of the substrate is unknown, take a blank measurement against air, with no sample or substrate in the light path. Then take a measurement of the substrate to determine the transmission spectrum of the material. After accounting for the air blank, the substrate spectrum can be subtracted from the transmission spectrum of the sample deposited on the substrate at a later time to correct for the transmission loss from the substrate.
- Ensure the film is facing the incident light beam. If the sample is facing the "wrong" direction, the light which interacts with the film may be attenuated by the substrate. For transmission measurements, the resulting spectrum will exhibit a lower %T than is expected in the regions where the substrate absorbs. In reflection measurements, attenuation by the substrate can also contribute to a loss of observed reflectance.
- If the thickness of the film is on the order of the wavelength of light used in the measurement (190 nm – 1100 nm for the Evolution Instruments), an interference pattern can be introduced in the spectrum as discussed previously. This pattern can be used to determine the thickness of the film; however, it can also obscure the true transmittance or reflectance spectrum of the material. Absorptive bands can dampen the effect of the interference, but complete removal of this interference pattern is difficult.
- For film samples, the deposited material is unable to rotate or "tumble" as it could in solution. This degree of freedom afforded to solution phase systems allows for the formation of an isotropic distribution of compounds present. As such, any light polarization dependencies will be averaged out as the molecules rotate in solution. In solids, polarization dependencies may be observed as the rigidity of a given molecule's orientation prevents averaging the observed impact of light polarization. Therefore, when working with a new material it can be helpful to measure the reflectance or transmittance in at least two different orientations to see if there is a polarization- or orientation-dependent effect present. This is particularly important for films which are highly ordered or crystalline in nature.

Conclusions

Though more complicated than solution-phase measurements, UV-Visible analysis of solid samples can provide valuable information about the behavior of a material. Herein, the use of UV-Visible transmission and reflection techniques was used to demonstrate effective analysis of powder, film and curved solid samples. To aid in these analyses, a variety of accessories compatible with the Evolution spectrophotometers can be used to measure powder or diffuse reflecting materials (ISA-220 and Praying Mantis) as well as determine the specular reflectance at multiple angles of incidence (VeeMAX variable angle specular reflectance accessory), including near-normal incidence (8˚ specular reflectance accessory).

References

1. Milosevic, M. S. L. B.; Beretsm S. L., A Review of FT-IR Diffuse Reflection Sampling Consiferations, *Appl. Spectrosc. Rev.*, **2002**, 37, 347-364.
2. Sellitto, V. M.; Fernandes, R. B. A.; Barrón, V.; Colombo, C. M., Comparing Two Different Spectroscopic Techniques for the Characterization of Soil Iron Oxides: Diffuse Versus Bi-Directional Reflectance, *Geoderma*, **2009**, 149, 2-9.
3. Shen, Y.; Hsu, C. W.; Yeng, Y. X.; Joannopoulos, J. D.; Soljačić, M., Broadband Angular Selectivity of Light at the Nanoscale: Progress, Applications and Outlook, *Appl. Phys. Rev.*, **2016**, 3, 011103.
4. Qu, Y.; Shen, Y.; Yin, K.; Yang, Y.; Li, Q.; Soljačić, M, Polarization-Independent Optical Broadband Angular Selectivity, *ACS Photonics*, **2018**, 5, 4125−4131.
5. Makula, P.; Pacia, M.; Macyk, W, How to Correctly Determine the Ban Gap Energy of Modified Semiconductor Photocatalysts Based on UV-Vis Spectra, *J. Phys. Chem. Lett.* **2018**, 9, 6814−6817.
6. Kapilashrami, M.; Zhang, Y., Liu, Y.-S.; Hagfeldt, A.; Guo, J., Probing the Optical Property and Electronic Structure of TiO_2 Nanomaterials for Renewable Energy Applications, *Chem. Rev.*, **2014**, 114, 9662-9707.
7. Zhao, Y.; Jia, X.; Waterhouse, G. I. N.; Wu, L.-Z.; Tung, C.-H.; O'Hare, D.; Zhang, T., Layred Double Hydroxide Nanostructured Photocatalysts for Renewable ENERGY Production, *Adv. Energ. Mater.*, **2016**, 6, 1501974.

Learn more at **thermofisher.com/evolution**

Application note

Analyzing Curved Surfaces with UV-Visible Techniques: Measuring Blue-Light Reductions Lenses

Introduction

Solid-state materials can be manufactured in a myriad of sizes and shapes. Often, the UV-Visible spectrum of these materials can provide valuable information about a substance's characteristics, including the color of a material or whether a material possesses the ability to block transmission of light at specific wavelengths. Solid phase samples, unlike solution phase samples, are able to reflect a non-negligible portion of incident light. Consequently, UV-Visible techniques are often employed to analyze not only the transmissive or absorptive properties of a sample, but the reflective properties as well.

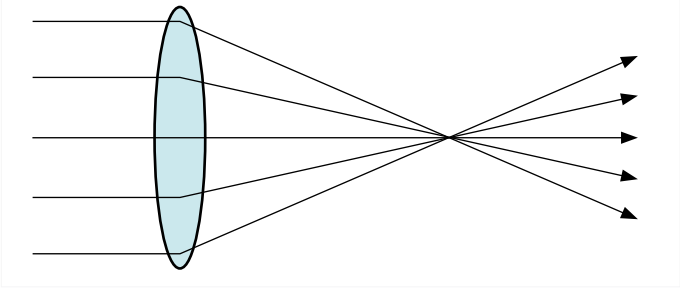

Figure 1. Light refraction from a focusing lens.

For materials which are curved or contain non-flat surfaces, refraction can cause light to be directed in a non-collimated fashion. This is the phenomenon which lenses utilize to allow for light to be focused or to diverge from the original collimated beam (Figure 1). These types of samples are often analyzed to learn more about a materials' transmissive and reflective behaviors in the UV-Visible spectral range. In traditional UV-Visible transmission measurements, a given sample is not expected to change the direction of the beam to a large degree; however, samples like lenses can alter the course of the beam significantly. This can lead to possible losses of transmitted light as the diverging beam is unable to be fully directed towards the detector.

To avoid possible errors in the collection of the true transmission spectrum, the addition of an integrating sphere accessory can aid in ensuring the transmitted light can reach the detector, resulting in an accurate transmission measurement. The interior of the sphere is coated with a highly reflective material to allow for the collection of light directed or scattered in non-uniform directions. The scattered light will diffusely reflect off the sphere walls many times until it is eventually able to reach the detector, which is held at an angle off the axis of the incident light beam (e.g., at 90° with respect to the incident beam).

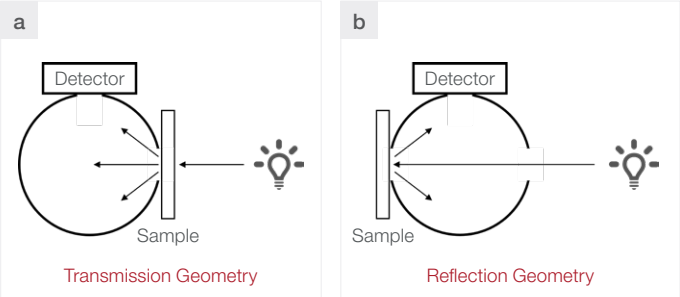

Figure 2. General diagram of an integrating sphere used in (a) transmission and (b) reflection geometry.

Due to the angle at which the detector is held, either reflectance or transmission measurements can be collected as shown in Figure 2. Through use of an integrating sphere, all light can theoretically be directed toward the detector, effectively eliminating issues posed by curved objects, diffuse reflectors or scattering substances. Owing to its ability to collect light directed off the beam axis and the versatility of the possible measurement geometries (reflection vs transmission), an integrating sphere is particularly useful for analysis of solid-state samples.

Blue light reduction glasses, a curved solid material, claim to reduce the amount of UV, violet and/or blue light which reaches the eye. The material in the lenses is intended to block the transmission of short wavelengths (UV: <400 nm, Violet: 400 – 440 nm, Blue: 440 – 500 nm) and transmit the remainder of the visible spectrum.[1,2] It is important that these lenses only block/reduce transmission at shorter wavelengths, allowing transmission at longer wavelengths. As a result, the measurement of the transmission spectrum is important for quality purposes. To demonstrate the ability to measure a curved surface, the transmission and reflectance spectra of a lens from a pair of violet/blue light reduction eyeglasses were measured using the Thermo Scientific™ Evolution™ One Plus spectrophotometer equipped with the Thermo Scientific ISA-220 integrating sphere (ISA-220). Through experiments described herein, the blocked UV-Visible range for a pair of violet/blue light reduction eyeglass lenses was found to be below 430 nm, indicating violet and UV light is blocked by the lens. However, these results indicate blue light can be transmitted through these lenses. Additionally, the absorptance spectrum of the lens was determined using the transmission and reflectance data. The absorptance spectrum was found to have a peak at 600 nm, matching the absorbance spectrum of the lens calculated from the measured transmission spectrum.

Experimental

A lens from a pair of violet/blue light reduction glasses was used as received. The material was measured using the Evolution One Plus UV-Visible spectrophotometer and ISA-220. Both % transmission (*%T*) and % reflectance (*%R*) spectra were collected, with the latter acquired using an 8° wedge to position the sample such that both diffuse and specular reflections were collected. A white Spectralon™ reference standard was used to establish the 100% reflectance baseline for the total reflectance measurements. This reference standard was also held at 8° with respect to the incident beam as well. The data was integrated for 0.1 s for each measurement.

Results/Discussion

Figure 3 includes both the transmission and total reflection spectrum of the eyeglass lens. The transmission spectrum starts to cut off at 430 nm and reaches 0% transmittance at 410 nm, indicating this lens is able to reduce violet light and below, however it does transmit blue light and above. At wavelengths longer than 430 nm, the transmission spectrum plateaus at ~90%, implying ~10 % of the light is unable to pass through the material. The remaining light can either be a result of absorption from the sample or from reflections. To better ascertain the origin of the unaccounted light, total reflectance measurements were acquired for the lens (Figure 3, red curve). Here, at wavelengths greater than 430 nm, ~10% of the incident light is reflected, accounting for the loss of transmitted light in this region.

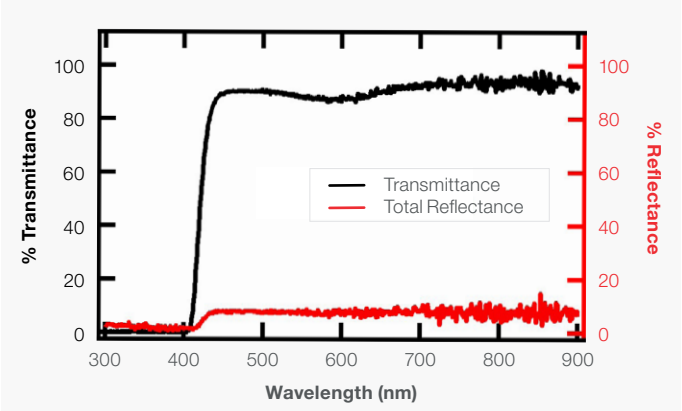

Figure 3. Transmittance (black) and Reflectance (red) spectra for a blue light reduction lens.

Additionally, in the transmission spectrum, a dip at 600 nm can also be observed. This dip is not present in the reflection spectrum, implying the lens or lens coating contains a material which absorbs in this region. As these lenses were commercially available, the source of this absorbance may either be intentionally included or is an unavoidable result due to the material used in the lens. However, it may be important to identify if an absorbing species is present and to what extent this species affects the optical transmission of the lens in the spectral region of interest.

By subtracting the transmittance and reflectance spectra from an assumed 100% light collection, the % absorptance of the material can be determined. Absorptance should not be confused with the more commonly referenced "absorbance" of a sample. While these terms are similar, the former includes the loss of light through reflections and transmission while the latter only accounts for the transmissive losses through Beer's law. Absorptance is typically reported using the same symbol as absorbance, A, but for the purposes of this note it shall be denoted as *%A*.

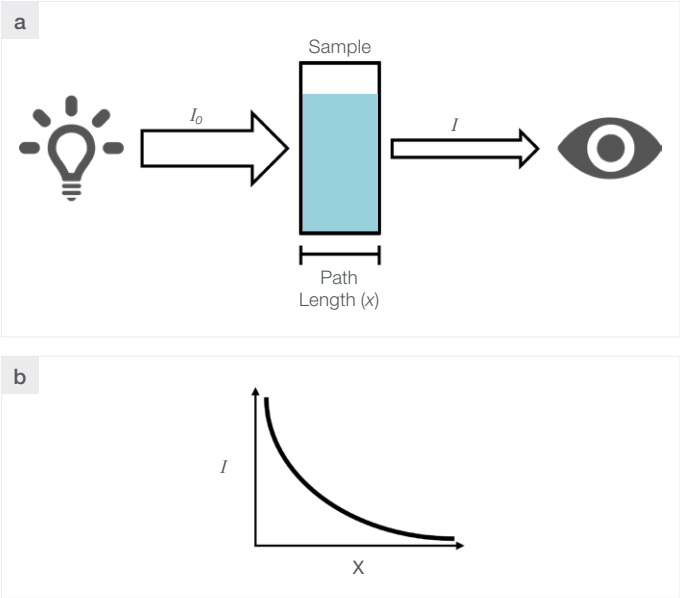

Figure 4. (a) Diagram depicting how incident light (I_0) is absorbed within a material, resulting in a lower intensity of remaining light (I) observed by the detector. (b) A depiction of the exponential relationship between the intensity of the light exiting the sample (I) and the path length (x).

Absorbance is calculated using equation 1, and is typically applied for liquid samples, where reflections are negligible, implying only transmissive losses exist.

$$A = \log\left(\frac{I_0}{I}\right) = \log\left(\frac{100}{\%T}\right)$$

Equation 1.

Here, I_0 is the intensity of the light before it interacts with the sample, and I is the intensity of the light that exits the sample through some given path length and *%T* is the percent transmission at a given wavelength. This is the form of Beer's law used by the spectrophotometer to determine the absorbance of a sample, and is visually represented through Figure 4, where I decays exponentially as a function of path length.

As absorbance is linear with respect to analyte concentration in solution, a linear function can be fit against a set of standards of known concentration. This technique makes quantification of an unknown concentration easy. From equation 1, it is shown that only the transmission of the material is accounted for, indicating any reflections or scattered light are, in effect, considered a part of the calculated absorbance term. For clear, non-turbid solutions, as has been discussed previously, these reflections and scattering events are considered negligible, allowing for this correlation between transmittance and absorbance to be accurate for solution phase samples.

Absorptance however, does not follow Beer's law and is not linear with changes to the concentration of the absorptive analyte. *%A* is related to the transmission and reflection spectra through the following equation,

$$100 = \%A + \%T + \%R$$

Equation 2.

where *%T* is the percent transmittance and *%R* is the percent total reflectance at a given wavelength. For solid-state materials, where reflections are non-negligible, this method is commonly reported.

Additionally, reporting *%A* can be helpful in applications in which the ratio of light absorbed by the sample is more important than quantifying the amount of a given analyte present in the sample matrix, such as solar energy applications.[3,4] For these applications, if the intensity of the light source is known, the absorptance can be used to determine the true intensity of incident light which is absorbed by the material. However, it is important to note that this is often an estimate as the *%R* spectrum is measured against a reference material (typically a mirror or diffuse reflectance standard). If the reference standard does not reflect 100% of the light, those losses will contribute to the calculated *%A* spectrum, though these differences are often negligible.

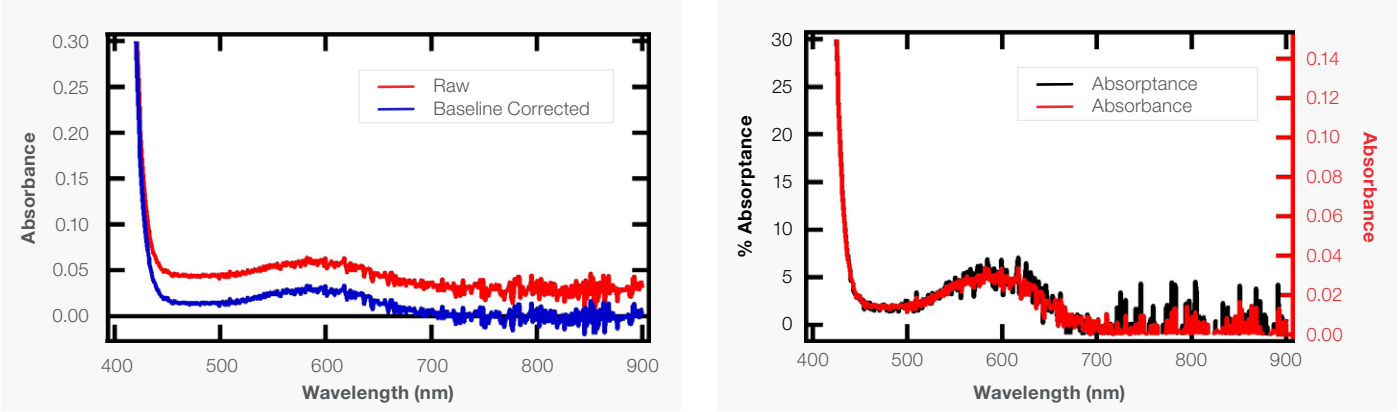

Figure 5. (a) Absorbance spectra (red - raw spectrum, blue - baselined corrected spectrum) of a blue light reduction lens. (b) Overlayed absorbance (red) and absorptance (black) spectra.

Absorbance and absorptance are very similar to one another, as is shown in Figure 5. Here, the calculated absorption spectrum (Figure 5a), taken by converting the percent transmission spectrum as shown in equation 1, can be shown to include a wide band with an absorption maximum centered at ~580 nm. The reflection spectrum for this material is significant, leading to an offset in the measured absorption spectrum. The contributions from reflections can be removed for this example by taking the average of the baseline (700 nm – 900 nm) and subtracting that value from the entire absorption spectrum.

Comparatively, the absorptance spectrum takes into account contributions from reflections. The resulting spectrum has a feature centered at ~580 nm as well. When scaled to match the maximum absorbance and absorptance, the spectra closely match one another (Figure 5b). While the value of the y-axis cannot be compared, the absorptance spectrum can be used to identify the spectral features present and compare to established absorption spectra of a given analyte.

Conclusions

Through the use of an integrating sphere, the experiments described herein demonstrate the ability to analyze the UV-Visible spectra of curved samples like lenses. The transmittance and reflectance spectra collected indicate the violet/blue light reduction glasses measured in this study prevent only violet and UV light from being transmitted. Additionally, the measurements included herein indicate a chromophore is present in the sample which absorbs at 600 nm, highlighting the ability to also calculate *%A* for solid materials in the UV-Visible range—a technique useful when analyzing samples when the fraction of light absorbed is more important to ascertain than the concentration of a given analyte.

References

1. Mainster, M.A., Intraocular Lenses Should Block UV Radiation and Violet but Not Blue Light, *Arch. Ophthalmol.*, **2005**, 123, 550–555.
2. Ali, A.; Roy, M.; Alzahrani, H. S.; Khuu, S. K, The Effect of Blue Light Filtering Lenses on Speed Perception, *Sci. Rep.*, **2021**, 11, 17583.
3. Liao, Q.; Zhang, P.; Yao, H.; Cheng. H.; Li, C.; Qu, L., Reduced Graphene Oxide-Based Spectrally Selective Absorber with an Extremely Low Thermal Emittance and High Solar Absorptance, *Adv. Sci.*, **2020**, 7, 1903125.
4. Palacios, A.; Calderón, A.; Barreneche, C.; Bertomeu, J.; Segarra, M.; Fernández, A.I., Study on Solar Absorptance and Thermal Stability of Solid Particles Materials Used as TES at High Temperature on Different Aging Stages for CSP, *Sol. Energy Mater Sol. Cells*, **2019**, 201, 110088.

Application note

Angle-Dependent Reflection Analysis of Smart Phone Privacy Screens

Introduction

From smart technology to solar cells, a variety of materials are analyzed as solid film samples. For some applications, analysis of these substances through UV-Visible spectroscopic techniques can be highly beneficial. Unlike liquid samples, solid samples are known to reflect a non-negligible amount of incident light. As such, it can be important to collect the reflection spectrum of a given sample for further materials characterization. These reflections can be either specular (mirror-like) or diffuse in nature (Figure 1). For film samples which do not appear opaque or cloudy, the reflection spectrum will be primarily specular while hazy films will mostly reflect light diffusely. For films which are clear to the naked eye, it is also possible to reliably measure the transmission spectrum as well, which can provide further insights into the behaviour of a given substance.

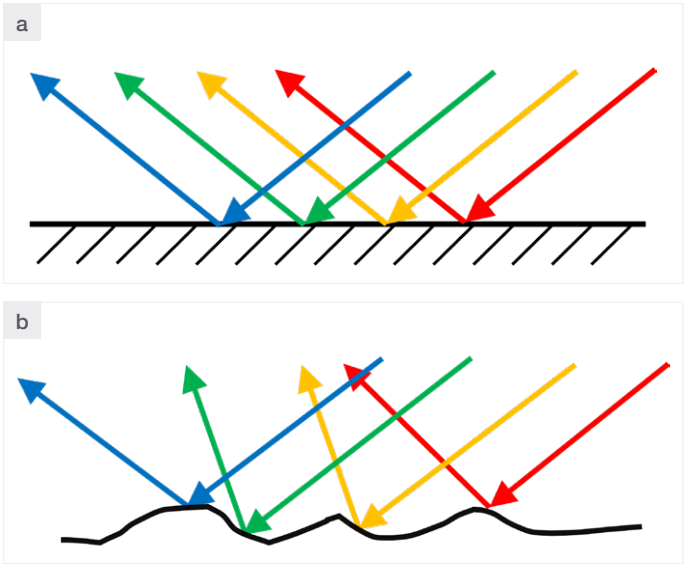

Figure 1. Diagrams depicting (a) specular and (b) diffuse reflections.

As an example, privacy screens for smart devices are films which protect the user's privacy by blocking light transmission when viewed from wide angles of incidence. These films typically utilize a micro-louvre design involving an array of "shades" which allows for transmission of light directed at a 0˚ angle of incidence.[1,2] At greater angles of incidence, the amount of light transmitted is limited. Similar methods have also been used for solar energy applications, like solar thermal collectors.[1,3]

Consequently, any privacy screen material will inherently have angle-dependent transmission and reflection spectra in the visible region of the electromagnetic spectrum. For quality purposes, it will be important to ensure that the screen blocks the full spectrum of visible light at a given angle with respect to normal incidence while allowing light to transmit when viewed directly. As light can either be transmitted, reflected or absorbed by a material, and given the privacy device is acting as a micro-louvre, behavior should be observed wherein more light is transmitted at smaller angles of incidence while less light is reflected at these angles. Therefore, it is important to measure the full transmittance and reflectance spectra as a function of the angle of incidence to ensure the film is behaving as expected.

Herein, the reflectance and transmittance spectra of a commercially available privacy screen were collected using the Thermo Scientific™ Evolution™ UV-Visible spectrophotometer. Reflection spectra were collected using multiple angles of incidence through the use of the Evolution Pro spectrophotometer equipped with the Thermo Scientific™ VeeMAX™ Variable Angle Specular Reflectance Accessory (SRA) and a fixed-angle 8˚ SRA. The Evolution One Plus instrument equipped with a Harrick Scientific Variable Angle Transmission holder was also used to collect the transmission spectra at varying angles of incidence.

thermo scientific

Experimental

A commercially available privacy screen compatible with smart phones was purchased and measured as received. For specular reflectance measurements, the Evolution Pro instrument was equipped with the appropriate SRAs. The percent reflectance (%R) spectrum was collected using 8˚, 30˚, 60˚, 70˚, and 80˚ angles of incidence. The data collected at an 8˚ angle of incidence was measured using the 8˚ SRA while the remaining measurements were collected using the VeeMAX Variable Angle SRA. Spectra were measured between 300 nm and 800 nm using a 1.0 nm step size, 1.0 nm bandwidth, and 0.1 s integration time. A reference mirror was used to establish the background.

Angle-dependent percent transmission (%T) measurements of the privacy screen were acquired using the Evolution One Plus. The Variable Angle Transmission holder was used to hold the screen at varying angles of incidence. For the data included herein the 0˚, 8˚, 30˚, 60˚, 70˚ and 80˚ angles of incidence were used. For transmission measurements, samples were measured twice with two different orientations: vertical and horizontal. The horizontal orientation, as its name implies, was achieved by rotating the sample 90˚ with respect to the vertical orientation. Similar to the reflectance data collected for this sample, spectra were measured between 300 nm and 800 nm using a 1.0 nm step size, 1.0 nm bandwidth, and 0.1 s integration time. The background was collected against air by using an empty holder.

Results/Discussion

As shown in Figure 2, the entirety of the specular reflectance spectrum for the privacy screen (Figure 2a) increases with rising angle of incidence while the opposite behavior is observed in the transmission spectrum (Figure 2b). Additionally, while the %R spectrum is almost flat across the entire measured range, the %T spectrum includes a feature with an onset at ~420 nm. This feature is likely due to some absorptive material within the film. The observations made imply, as expected, that when viewed directly (normal or smaller angles of incidence) the privacy screen has greater light transmission and less reflections than if viewed at larger angles of incidence.

It should be noted that both %R and %T spectra collected for the sample held at an 8˚ angle of incidence (and 0˚ for the transmission measurements) include an interference pattern (Figure 2). Interference patterns look like oscillations across the UV-Visible spectrum and are observed when the thickness of the film is on the order of the wavelength of light used in the measurement.[4] Under these conditions, the light which reflects off the air/film interface and the film/substrate interface constructively and destructively interfere with one another, leading to the observed interference pattern. This phenomenon occurs when the various interfaces are uniform or have minimal roughness[5] and has been reported previously for a variety of thin film samples.[4-7] In terms of the privacy screen, the observed interference pattern implies the sample contains a film deposited on the substrate which is hundreds of nm thick. Furthermore, this pattern also implies the film is relatively uniform.

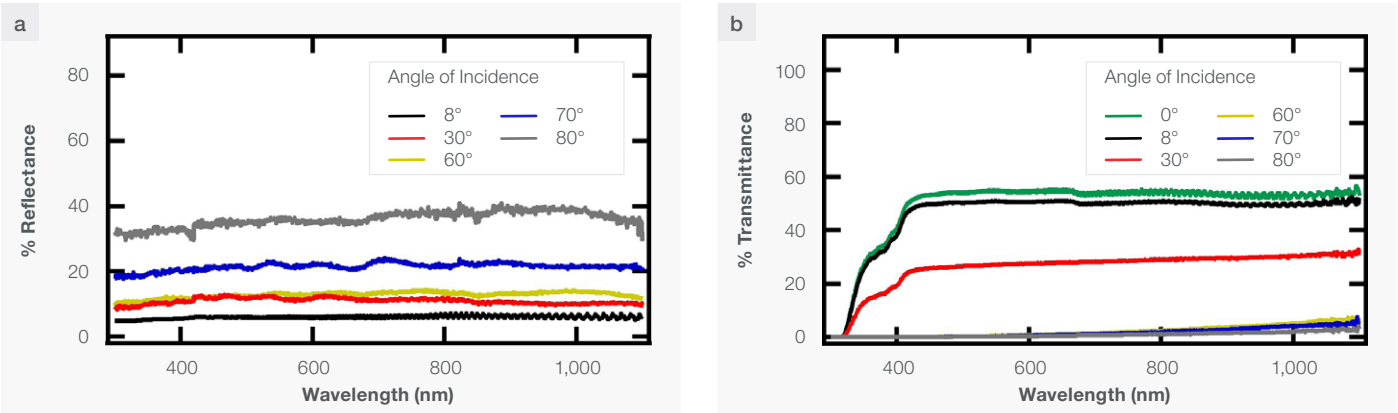

Figure 2. (a) Specular Reflectance and (b) transmittance spectra of a privacy screen collected at different angles of incidence.

Figures 3a and 3b include %T spectra collected using 0˚ and 80˚ angles of incidence, respectively. %T measurements of the privacy screen were also collected at two different orientations: vertical (Figure 3c) and horizontal (Figure 3d). As is shown, the sample held at a vertical orientation transmits less light, regardless of the angle of incidence, than if the sample were positioned horizontally. Given this screen is made for a smart phone, where the device is commonly held vertically, this behavior meets expectation that less light is transmitted when viewed under this orientation, especially at wide angles.

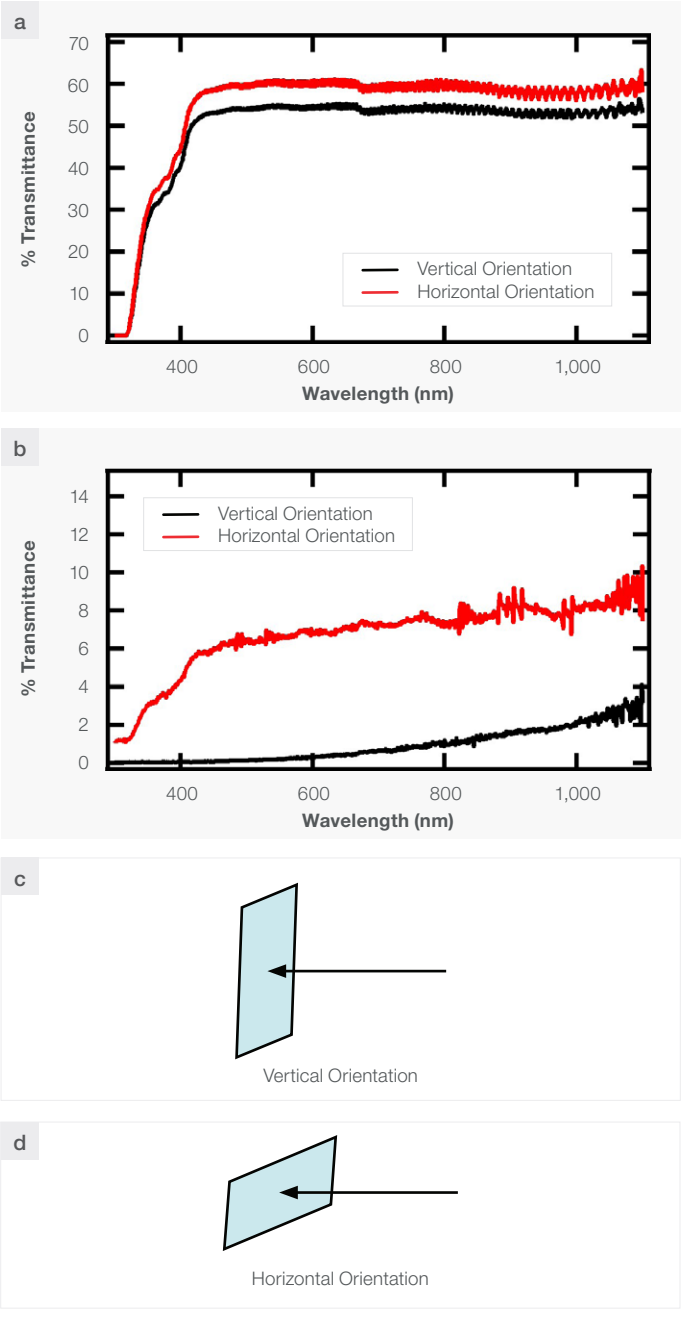

Figure 3. Orientation dependence of the transmission spectrum of a privacy screen oriented vertically (black) or horizontally (red). The sample was measured using a (a) 0˚/normal and (b) 80˚ angle of incidence. Diagrams depicting the difference between vertical (c) and horizontal (d) orientation. For both diagrams, the arrow indications the direction of the incident beam.

The orientation dependence of the privacy film sample is similar to the behavior a polarizer exhibits. A polarizer is an optical component often used in spectroscopic measurements. Polarizers allow light of a given polarization to pass through while rejecting light of different polarizations. These materials are highly orientation dependent, such that rotating the polarizer changes the allowed transmittable polarization (Figure 4).

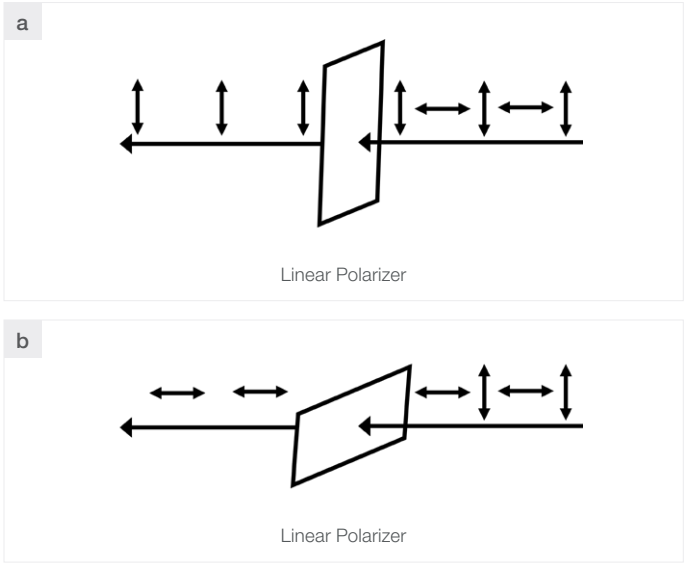

Figure 4. Depiction of how a polarizer only allows light of a specific polarization to transmit. As is shown, the orientation of the polarizer affects what polarization is allowed to pass.

In the context of samples, polarization can also have an impact on the measured absorption spectrum. For both solution- and solid-phase samples, molecules can absorb light of varying polarizations differently. Often, this behavior is dependent on the molecule's orientation.[8] The ability for molecules to "tumble" in solution effectively allows for the sample to remain isotropic. This behavior prevents orientation effects from influencing the overall measured spectrum. However, polarization dependence can be present in a variety of solid-state samples where the compounds cannot freely rotate like they would in solution. Because this degree of freedom is lost for solids, the orientation of the compounds within the matrix can affect the measured spectrum; rotating the sample can change the observed spectrum. As a result, it is generally helpful when analyzing solid-state samples to collect data at more than one sample orientation as a check to determine if perceived differences in spectra are a product of polarization-dependence.

Conclusions

Herein, the ability to measure %R and %T spectra of film samples at varying angles of incidence was demonstrated using the Evolution instruments with appropriate accessories. By increasing the angle of incidence, the %R spectrum was found to increase while the %T spectrum was found to increase, meeting the expected results for the privacy screen. Furthermore, the orientation dependence observed highlights the need to ensure solid-state samples are reproducibly placed when measured.

References

1. Shen, Y.; Hsu, C. W.; Yeng, Y. X.; Joannopoulos, J. D.; Soljačić, M., Broadband Angular Selectivity of Light at the Nanoscale: Progress, Applications and Outlook, *Appl. Phys. Rev.*, **2016**, 3, 011103.
2. Qu, Y.; Shen, Y.; Yin, K.; Yang, Y.; Li, Q.; Soljačić, M, Polarization-Independent Optical Broadband Angular Selectivity, *ACS Photonics*, **2018**, 5, 4125−4131.
3. Evangelisti, L.; Vollaro, R. D. L.; Asdrubali, F., Latest Advances on Solar Thermal Collectors: A Comprehensive Review, *Renewable Sustainable Energy Rev.*, **2019**, 114, 109318.
4. Huibers, P. D. T.; Shah, D. O., Multispectral Determination of Soap Film Thickness, *Langmuir*, **1997**, 13, 5995-5998.
5. Larena, A.; Millán, F.; Pérez, G.; Pinto, G., Effect of Surface Roughness on the Optical Properties of Multilayer Polymer Films, *Appl. Surf. Sci.*, **2002**, 187, 339-346.
6. Mohanty, P.; Rath, C.; Mallick, P.; Biswal, R.; Mishra, N. C., UV-Visible, Studies of Nickel Oxide Thin Film Grown by Thermal Oxidation of Nickel, *Physica B*, **2010**, 405, 2711-2714.
7. Choudhari, K. S.; Kulkarni, S. D.; Unnikrishnan, V. K.; Sinha, R. K.; Santhosh, C.; George, S. D.; Optical Characterizations of Nanoporous Anodic Alumina for Thickness Measurements Using Interference Oscillations, *Nano-Struc. Nano-Objects*, **2019**, 19, 100354.
8. Nordén, B., Applications of Linear Dichroism Spectroscopy, *Appl. Apectrosc. Rec.*, **1978**, 14, 157 – 248.

Learn more at **thermofisher.com/evolution**

Application note

Band Gap Analysis through UV-Visible Spectroscopy

Introductions

Semiconducting materials are often analyzed using UV-Visible spectroscopy to learn more about the electronic structure of the substances.[1-3] For semiconductors, the electronic structure is not defined in the same manner that small molecules are described. In these materials, the electronic states are clustered very close in energy to one another, resulting in a band of electronic states instead of discrete energy levels. The highest filled energy band, analogous to the highest occupied molecular orbital (HOMO) for small molecules, is referred to as the valence band (VB); the lowest unoccupied energy band, similar to the lowest unoccupied molecular orbital (LUMO) in molecules, is referred to as the conduction band (CB).[4]

The top of the VB and bottom of the CB in semiconductors are separated by an energy gap, referred to as the band gap (E_g) as shown in Figure 1.[4,5] Unlike metals, where electrons can freely move, this separation in semiconductors prevents the transfer of electrons to the conduction band under standard conditions. Electrons occupying the VB can be promoted to the CB given enough energy is supplied to equal or surpass E_g. This can be accomplished through either applying a potential across the material or through irradiation of the material with the appropriate wavelength of light.

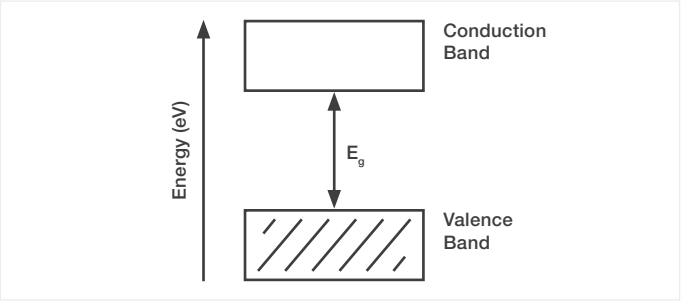

Figure 1. General electronic structure for semiconducting materials. Eg refers to the band gap energy and is typically reported in eV units.

Information about the electronic structure of the material can be important to determine, as this can have ramifications for photo-induced processes within the material like photocatalysis[6] or solar energy conversion.[2] In combination with other methods, such as electrochemical analysis (e.g., cyclic voltammetry),[7] ultraviolet photoelectron spectroscopy (UPS)[8], and computational calculations,[2] this information can be used to understand the position of the CB and VB relative to a standard electrode reference. Because UV-Visible absorption and reflectance spectra arise from transitions between occupied and unoccupied states, these spectral measurements can be directly used to estimate E_g.

Traditionally, the band gap energy is determined through use of a Tauc analysis, by which the band gap energy is related to the absorption coefficient through the following equation,

$$(\alpha h\nu)^{\frac{1}{\gamma}} = B(h\nu - E_g)$$

Equation 1.

where α is the absorption coefficient, h is Plank's constant (6.63×10^{-34} J•s), ν is the frequency of the incident photon, γ is a parameter reflecting the nature of the band gap transition (e.g., direct/indirect, allowed/forbidden), B is the slope of the linear portion of the Tauc Plot and E_g is the band gap energy.[1,9,10] The Tauc plot is constructed by reporting the collected spectrum as $\alpha h\nu^{(1/\gamma)}$ vs. Energy (eV). As absorbance is proportional to α through Beer's law, the collected absorbance can be used in place of the absorption coefficient to develop the curve. The energy axis is determined by converting the analyzed wavelength spectrum to energy through equation 2,

$$E = \frac{hc}{\lambda}$$

Equation 2.

where E is the converted energy, c is the speed of light (3.0×10^8 m/s), h, as before, is Plank's constant and λ is the wavelength of light. By convention, the calculated energy is converted from J to eV. From the curve, a tangent line can be fit to the linear section of the data. The intersection of the tangent line with the x-axis denotes the estimated band gap energy of the material.

If the material can be suspended in a liquid and results in an optically clear, non-turbid solution, then the measured absorbance of the colloidal solution can be used in the Tauc plot analysis.[9] However, for powders and non-transparent solid samples reflectance measurements are the appropriate method for analysis. Due to the irregularity of the surface of particles within the powder or thin films, these reflections are primarily diffuse in nature, implying there are likely fewer specular reflections observed. Diffuse reflections are often directed at multiple different angles, including away from the detector, leading to an unintentional omission of reflections during the experiment.

To avoid this issue, an integrating sphere can be used to collect all light reflected by the material. As implied by its name, the interior of this accessory is spherical and coated with a highly reflective substance. When light diffusively reflects off the sample, the reflections bounce of the interior coating many times until it is directed towards the detector. Without the sphere, these diffuse reflections would not be able to reach the detector and would not be included in the reflectance spectrum. Alternatively, diffuse reflectance accessories, like the Thermo Scientific™ Praying Mantis™ Diffuse Reflectance Accessory, can also be used to collect the diffuse reflections without the use of an integration sphere.

Under circumstances where thin films or powdered semiconducting samples are studied, the diffuse reflectance spectrum can be collected and reported in place of absorbance using the Kubelka-Munk formulism (equation 3),

$$F(R) = \frac{(1-R)^2}{2R}$$

Equation 3.

where *F(R)* is the Kubelka-Munk value (unitless), and *R* is the collected percent reflectance (%R) of the sample as a function of wavelength.[1,10] *F(R)* is directly proportional to the absorption coefficient according to equation 4,

$$F(R) = \frac{k}{s}$$

Equation 4.

where *k* is the absorption coefficient, and *s* is the scattering coefficient.[3,12] Using this transformation in place of α, the Tauc plot can be constructed for powder and film samples, allowing for a determination of E_g.

As an example, the reflectance spectrum of two powdered TiO_2 samples of differing crystal structure (rutile and anatase), both well- characterized semiconducting materials,[11,12] were acquired using the Thermo Scientific™ Evolution™ One Plus UV-Visible Spectrophotometer, equipped with an ISA-220 Integrating Sphere, and an appropriate powder sample holder. Similarly, the same experiment was performed using the Thermo Scientific™ Evolution™ Pro UV-Visible Spectrophotometer and the Praying Mantis diffuse reflectance accessory. Through the collected spectra, Tauc plots were generated and compared between both instruments. The resulting E_g for each respective sample not only match using measurements acquired on different instruments, but also agree with literature, demonstrating the ability to quickly analyze the bandgap energy of solid-state semiconductors through the analysis of UV-Visible spectra.

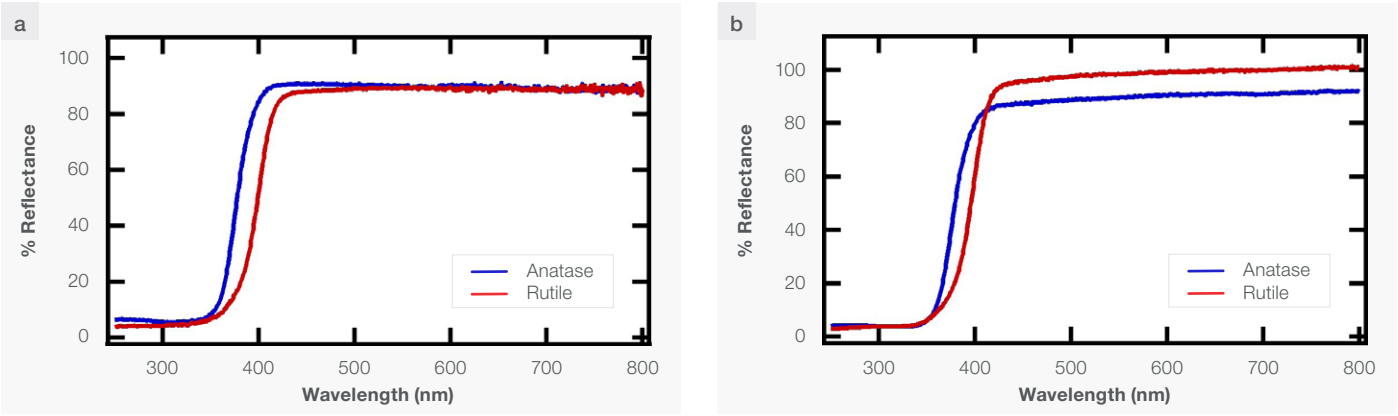

Figure 2. Diffuse reflectance spectra of anatase (blue) and rutile (red) TiO_2. Spectra were collected using (a) the ISA-220 integrating sphere and (b) the Praying Mantis diffuse reflectance accessory.

Experimental

Both anatase and rutile TiO_2 samples were measured as received using the Evolution One Plus equipped with an integrating sphere (ISA-220) and the Evolution Pro with the Praying Mantis. For data collected using the Evolution One Plus and ISA, the sample was held in a powder sample holder and measured without using an 8° wedge, allowing for collection of only diffuse reflections. With both accessories, the %R spectrum was collected between 250 nm and 800 nm using a 1.0 nm bandwidth and 1.0 nm step size. The data was integrated for 0.25 s using the Praying Mantis and for 0.5 s using the ISA-220. The background was collected using a white Spectralon reference material for measurements collected using the ISA-220, while a PTFE diffuse reflectance disk was used for measurements collected using the Praying Mantis.

Results/Discussion

To demonstrate this analysis, the %R spectra of two different TiO_2 nanoparticles of different crystal structure, anatase and rutile, were measured using the Evolution One Plus. As these samples were analyzed in powder form, the ISA-220, an integrating sphere accessory, was used. As can be seen in the reflectance spectra in Figure 2a, both TiO_2 samples do not reflect a substantial amount of UV light below 350 nm, however the onset observed for rutile is at a slightly longer wavelength than for the anatase TiO_2 sample. As the wavelength and energy of a photon is inversely proportional according to equation 2, this implies that the bandgap energy is likely smaller for the rutile TiO_2 sample than for the anatase sample.

For samples with limited amount of material, the Praying Mantis Diffuse Reflectance Accessory can also be used for the same analysis. This accessory allows for the measurement of diffuse reflections of powder substance. These materials can be held in sample holders with a total volume of 250 mm^3 (macro holder) or 31.6 mm^3 (micro holder). Unlike an integrating sphere, this accessory only collects the diffuse reflections from a material. Additionally, this apparatus can be used in tandem with a reaction chamber to provide an inert environment, introduce reaction gases to the powdered sample, or control the temperature of the material. This can be particularly helpful for *in-situ* analysis of the UV-Visible reflectance spectrum of materials used in high-temperature catalytic reactions held at the appropriate temperature.

The same diffuse reflectance measurements were performed using the Evolution Pro and Praying Mantis, as reported in Figure 2b. The data collected shows a similar trend as the measurements acquired using the integrating sphere. A minimal amount of light below 350 nm is reflected for both samples, while the onset for rutile TiO_2 begins at a longer wavelength than the onset for anatase TiO_2. However, at longer wavelengths, the %R recorded for both samples do not appear to perfectly match when comparing measurements collected with the integrating sphere and Praying Mantis accessories.

It is important to note that the %R spectra collected using the integrating sphere or Praying Mantis are relative measurements, not absolute. This is due to the method used to determine the initial intensity of the light prior to interacting with the sample. Because a standard such as Spectralon or PTFE is required to establish the initial light intensity, the %R will be dependent on how well the standard reflects light. As such, measuring samples using different reflectance standards can result in slight variations in overall measured spectrum intensity, especially in regions where most or all of the light is reflected by the sample. Additionally, variations in the Y-axis may arise as a result of variations in the amount of material probed due to differences in the angle of incidence between the two accessories.

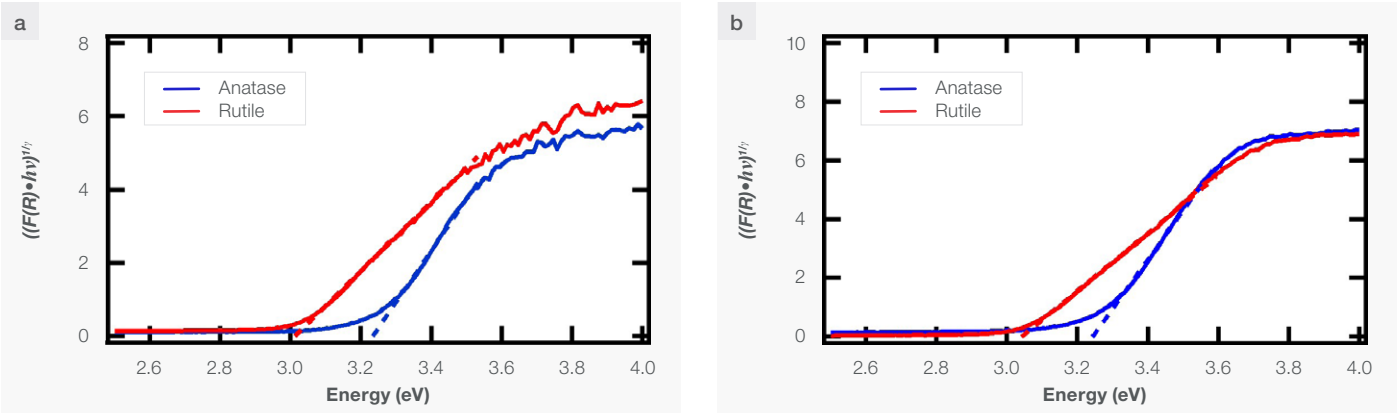

Figure 3. Tauc Plot for rutile (red) and anatase (blue) TiO_2 collected using (a) an integrating sphere and (b) the Praying Mantis diffuse reflectance accessory. The dashed lines are the tangent lines fit to the linear portion of the spectrum. As TiO_2 has an indirect band gap, $\gamma = 2$.

Using the methodology described earlier, Tauc Plots were constructed from the reflectance measurements for these samples (Figure 3). TiO_2 has been extensively studied and has a well-defined indirect band gap for both crystal structures analyzed herein. From the Tauc analysis, E_g was found to be 3.23 ± 0.06 and 3.01 ± 0.02 for anatase and rutile TiO_2, respectively based on data measured using the integrating sphere, as shown in Table 1. Similar E_g were calculated using data collected with the Praying Mantis diffuse reflectance accessory as well (Table 1), indicating consistent results can be acquired using both accessories. Both sets of calculated band gap energies are consistent with literature results as well[11,12] demonstrating both the integrating sphere and Praying Mantis can be reliably used for this application.

	Band gap energy (eV)	
	Integrating sphere	Praying mantis
Anatase TiO_2	3.23 ± 0.06	3.24 ± 0.05
Rutile TiO_2	3.01 ± 0.03	3.04 ± 0.02

Table 1. Calculated band gap energies for anatase and rutile TiO_2 determined from data collected using an integrating sphere (ISA-220) and the Praying Mantis diffuse reflectance accessory.

Conclusions

In this study, the Evolution UV-Visible spectrophotometers were used to acquire reflectance spectra for TiO_2 samples of varying crystal structure. Through use of the Tauc Plot analysis, the band gap energy was found to be approximately 3.0 eV and 3.2 eV for the rutile and anatase TiO_2 samples, respectively, matching literature values. The calculated band gap energy matched well for measurements collected with both the integrating sphere and Praying Mantis accessories, demonstrating reliability and consistency between the two methods. Though care should be taken when comparing samples measured using different baseline reflectance standards, the results included herein exhibit the ability to effectively analyze solid-state materials using the Evolution instruments and associated accessories.

References

1. Makula, P.; Pacia, M.; Macyk, W, How to Correctly Determine the Ban Gap Energy of Modified Semiconductor Photocatalysts Based on UV-Vis Spectra, *J. Phys. Chem. Lett.* **2018**, 9, 6814–6817.
2. Kapilashrami, M.; Zhang, Y., Liu, Y.-S.; Hagfeldt, A.; Guo, J., Probing the Optical Property and Electronic Structure of TiO_2 Nanomaterials for Renewable Energy Applications, *Chem. Rev.*, **2014**, 114, 9662-9707.
3. Zhao, Y.; Jia, X.; Waterhouse, G. I. N.; Wu, L.-Z.; Tung, C.-H.; O'Hare, D.; Zhang, T., Layred Double Hydroxide Nanostructured Photocatalysts for Renewable ENERGY Production, *Adv. Energ. Mater.*, **2016**, 6, 1501974.
4. Atkins, P., Shriver & Atkins' Inorganic Chemistry, Oxford University Press, 2010.
5. Weller, P. F.; An Analogy for Elementary Band Theory Concepts in Solids, *J. Chem. Ed.*, **1967**, 44, 391-393.
6. Kisch, H.; Macyk, W., Visible-Light Photocatalysis by Modified Titania, *ChemPhysChem*, **2002**, 3, 399-400.
7. Inamdar, S. N.; Ingole, P. P.; Haram, S. K., Determination of Band Structure Parameters and the Quasi-Particle Gap of CdSe Quantum Dots by Cyclic Voltammetry, *ChemPhysChem*, **2008**, 9, 2574-2579.
8. Jasieniak, J.; Califano, M.; Watkins, S. E., Size-Dependent Valence and Conduction Band-Edge Energies of Semiconductor Nanocrystals, *ACS Nano*, **2011**, 5, 5888-5902.
9. Coulter, J. B.; Birnie, D.P.; Assessing Tauc Plot Slope Quantification: ZnO Thin Films as a Model System, *Phys. Status Solidi B*, **2018**, 255, 1700393.
10. López, R.; Gómez, R., Band-Gap Energy Estimation from Diffuse Reflectance Measurements on Sol-Gel and Commercial TiO_2: A Comparative Study, *J. Sol-Gel Sci. Technol.*, **2012**, 61, 1-7.
11. Nosaka, Y.; Nosaka, A. Y., Reconsideration of Intrinsic Band Alignments within Anatase and Rutile TiO_2, *J. Phys. Chem. Lett.*, **2016**, 7, 431-434.
12. Miao, L.; Jin, P.; Kaneko, K.; Terai, A.; Nabatova-Gabain, N.; Tanemura, S, Preparation and Characterization of Polycrystalline Anatase and Rutile TiO_2 Thin Films by Rf Magnetron Sputtering, *App. Surf. Sci.*, **2003**, 212, 255-263.

Learn more at **thermofisher.com/evolution**

Notes

Learn more at **thermofisher.com/evolution**

thermo scientific